Cascade Analysis of a Floating Wind Turbine Rotor

2014 J. Phys.: Conf. Ser. 555 012053

(http://iopscience.iop.org/1742-6596/555/1/012053)

Cascade Analysis of a Floating Wind Turbine Rotor

Lene Eliassen[1], Jasna B. Jakobsen[1], Andreas Knauer[2], Finn Gunnar Nielsen[2]

[1]Department of Mechanical and Structural Engineering and Materials Science, University of Stavanger, [2] Statoil

E-mail: lene.eliassen@uis.no

Abstract. Mounting a wind turbine on a floating foundation introduces more complexity to the aerodynamic loading. The floater motion contains a wide range of frequencies. To study some of the basic dynamic load effect on the blades due to these motions, a two-dimensional cascade approach, combined with a potential vortex method, is used. This is an alternative method to study the aeroelastic behavior of wind turbines that is different from the traditional blade element momentum method. The analysis tool demands little computational power relative to a full three dimensional vortex method, and can handle unsteady flows.

When using the cascade plane, a "cut" is made at a section of the wind turbine blade. The flow is viewed parallel to the blade axis at this cut. The cascade model is commonly used for analysis of turbo machineries. Due to the simplicity of the code it requires little computational resources, however it has limitations in its validity. It can only handle two-dimensional potential flow, i.e. including neither three-dimensional effects, such as the tip loss effect, nor boundary layers and stall effects are modeled. The computational tool can however be valuable in the overall analysis of floating wind turbines, and evaluation of the rotor control system.

A check of the validity of the vortex panel code using an airfoil profile is performed, comparing the variation of the lift force, to the theoretically derived Wagner function. To analyse the floating wind turbine, a floating structure with hub height 90 m is chosen. An axial motion of the rotor is considered.

1. Introduction

The wind resources offshore are stronger, less turbulent and more predictable relative to the onshore wind resources. In the shallow water areas outside Denmark, Germany and Great Britain there are large offshore wind turbine parks in operation, but the wind turbine development is still very limited for deeper waters. The trend is that the wind turbines are installed further from the coast and at larger water depth. At the end of 2011, the offshore wind turbines' installed capacity was 3 812 MW, but only 2 out of 1371 offshore wind turbines were full scale floating wind turbines [1].

Figure 1 illustrates the development from onshore to offshore in wind turbine technology. In deep waters it is not economically practical to have the wind turbines fixed to the seabed, and a floating alternative is needed. Some of the areas with high wind speed have deep waters and one needs floating wind turbines to capture the wind energy. The area outside the western coast of Norway is such an example. Outside the west coast of Norway, Statoil has deployed a floating wind turbine, similar to the floater in figure 2. This wind turbine has been successfully operating since autumn 2009 [2].

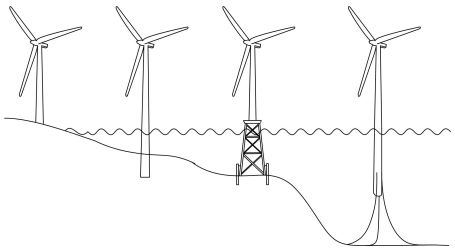

Figure 1. The technology as it is developed from onshore wind turbines and to floating wind turbines.

The aerodynamics of a conventional bottom fixed horizontal axis wind turbine can be computed by applying the blade element momentum (BEM) method [3]. However, a floating wind turbine, will have additional rigid body degrees of freedoms (DOFs) and this introduces more complexity in the aerodynamic loading. The additional DOFs are shown in figure 2. The six DOFs illustrated in figure 2 are both translational and rotational motion. The rotational motions are termed pitch (y-axis), yaw (z-axis) and roll (x-axis), and the translational motions are termed heave (z-axis), surge (x-axis) and sway (y-axis).

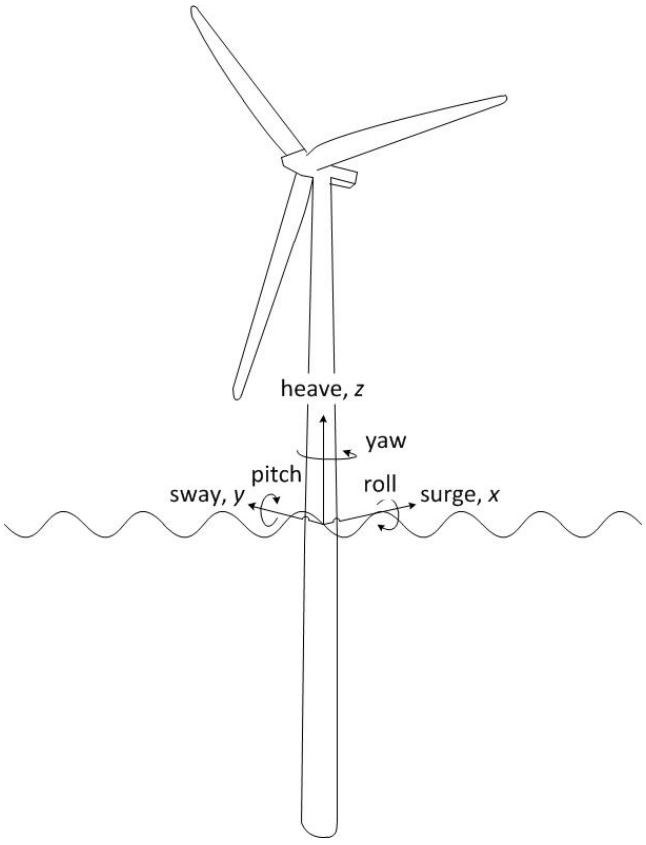

Figure 2. Offshore floating wind turbine platform degrees of freedom.

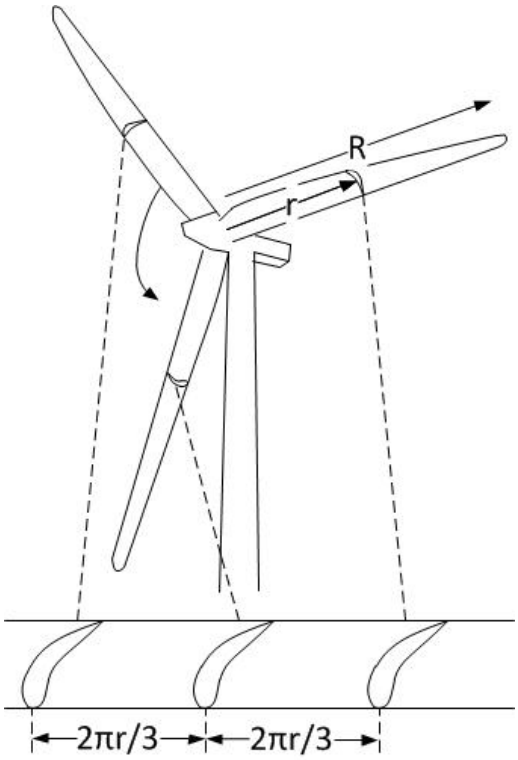

Figure 3. Transformation of blade element into cascade configuration.

The studies of floating wind turbines often assumes that the BEM method is valid, even with the additional rigid body DOFs introduced. The BEM method is based on momentum theory [3]. However, when the floating wind turbine is operating in wind conditions which are below rated wind speed, the momentum balance may break down. The reason for this is that the contribution to the effective wind speed due to the platform motions are relatively larger for

lower wind speeds [4]. For wind speeds at rated or above rated the momentum balance may be sufficient to be used. The DOFs, which are most significant for aerodynamics of a floating HAWT, have been discussed in [4]. For a spar-buoy type of platform, as shown in figure 2, the DOFs that may lead to unsteady loading are pitch and yaw.

As an alternative to the commonly used BEM method, we have analysed the aerodynamics of the rotor using a simple 2D vortex panel method. The advantage of using the panel method is that it does not need aerodynamic load coefficient a priori. Since the panel code includes the vorticity in the wake, a good estimation of the transient aerodynamic loads is obtained. Instead of modelling only a single airfoil, a cascade of airfoils is modelled. In the cascade the adjacent airfoils are included in the analyis of the aerodynamic loads. The method used will show how the thrust force will be affected by the platform motions. The analysis will investigate the rotor-flow interaction due to an axial motion of the rotor. This axial motion will occur as a combined pitch and surge motion of the floating foundation.

2. Theory

The aerodynamic analysis method presented in this section is based on the following assumptions:

- The fluid is incompressible, irrotational and inviscid, i.e. potential flow.
- There is no flow in the meridional plane, only in the cascade plane, i.e. there is no flow from one radial cross section to another.

These assumptions limit the validity of our analysis. As a consequence to the flow being inviscid, the stall effect is not modeled. This is the largest weakness of the potential vortex method, as the stall effect is important to the loading of the airfoil. If the flow in the meridional plane is neglected, the flow along the blade is assumed zero. This is erroneous, especially close to the tip of the wind turbine blade, where there is a tip loss effect. The tip loss effect can be included in the simulations by a correction factor, such as the Prandtl method. The Prandtl method is often used to include the tip loss effect in BEM methods, which have the same limitations as our cascade analysis with regards to two dimensional flow [3].

2.1. Cascade aerodynamics

The cascade theory is applied to a two-dimensional airfoil. The thrust force from the aerodynamic load can be estimated by integrating the normal force over the length of the blade. The transformation of a blade element of a wind turbine into a cascade configuration is shown in figure 3. The blade elements are presented as a cascade of airfoils and the distance between airfoil sections is the circumference of the rotor at the blade section, divided by the number of blades.

The incoming velocity is a result of the velocity through the wind turbine plane of rotation and a rotational component of the wind turbine. A velocity diagram is shown in figure 4.

2.2. Vortex panel methods

It can be shown that the velocity potential of the potential flow can be described by the Laplace's equation [5]. Singular elements, which are solutions of the Laplace's equation, are used to describe the flow. The singular elements are distributed along the airfoil surface and the wake. The strength of the singular elements are found enforcing boundary conditions along the surface of the airfoil and the wake.

2.2.1. Procedure. The sequence to set up the vortex panel method is as follows [5]:

(i) Selection of singularity element

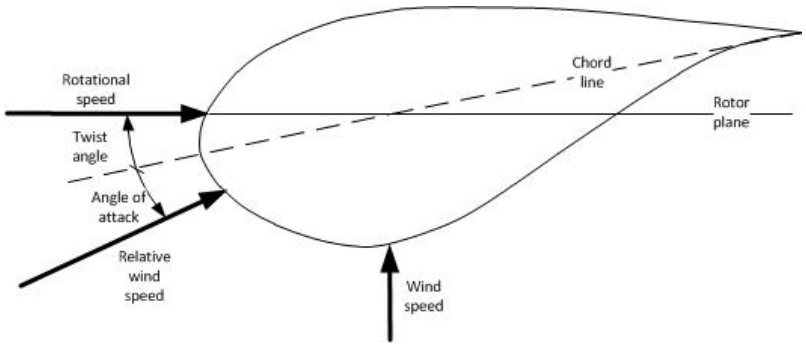

Figure 4. An illustration of an airfoil and the flow velocities included in the simulation.

(ii) Discretization of geometry
(iii) Determination of influence coefficient
(iv) Establishment of the RHS of the equation
(v) Solution of the linear set of equation

The main steps will be described in detail in the order listed. The time-stepping procedure will be presented after the main steps have been presented. At the end of this section, the calculation of the lift force will be shown.

2.2.2. Selection of singularity element. In the vortex panel method the flow field is modeled by a combination of singular elements. On the airfoil, the surface is divided into linear segments with sources and doublets of constant strength. The wake is modeled with linear panels with constant doublet strength. The difference in velocity potential at a point P, located at (x, y), due to a constant two dimensional strength source is defined by [5]:

$$\Delta\Phi_S = \frac{\sigma}{4\pi}\{(x-x_1)\ln[(x-x_1)^2+z^2]-(x-x_2)\ln[(x-x_2)^2+z^2]+2z(\tan^{-1}\frac{z}{x-x_2}-\tan^{-1}\frac{z}{x-x_1})\} \quad (1)$$

where σ is the strength of the source element with end points x_1, z_1 and x_2, z_2. A local coordinate system is used, where the x-axis is along the panel element and the origin is at the first end point of the panel, (x_1, y_1). Similarly, the difference in the potential due to the constant strength doublet is defined by [5]:

$$\Delta\Phi_D = \frac{-\mu}{2\pi}[\tan^{-1}\frac{z}{x-x_2} - \tan^{-1}\frac{z}{x-x_1}] \quad (2)$$

where μ is the strength of the doublet element.

2.2.3. Discretization of geometry. The geometry of the airfoil is discretized into linear elements. Special attention should be paid at the trailing edge and at the leading edge to get the correct discretization in these areas. The discretization of an airfoil is illustrated in figure 5. A collocation point is located at the center of each panel element.

2.2.4. Determination of influence coefficient. The influence coefficients are defined as the change in velocity potential at the collocation point of panel element i, due to the singular strength of panel element j. The strength of the singular elements are set to 1, when calculating the influence coefficients. The collocation point is located in the middle of the panel element i, at x_{ci}, y_{ci}. The influence coefficient at panel element i, due to the source panel element, j, located along the airfoil surface is denoted B_{ij} and is calculated by Equation 1. The influence

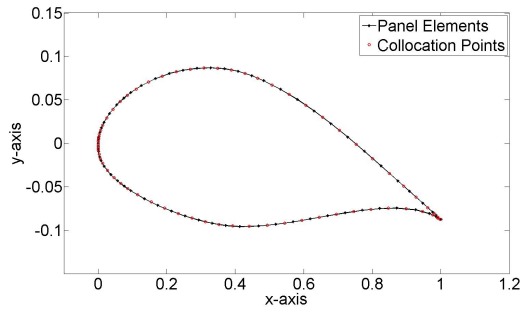

Figure 5. Approximation of the airfoil surface by panel elements.

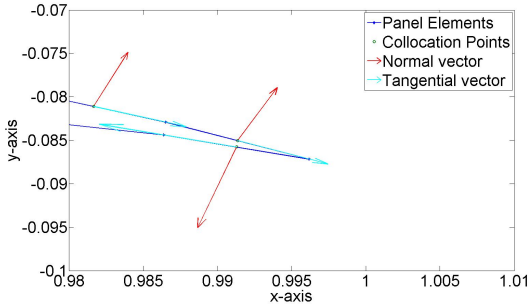

Figure 6. The two first and last panel elements with collocation point, local normal and tangential vector.

coefficients due to the doublet panel elements along the surface are denote C_{ij}, and in the wake C_{il}, and are both calculated by Equation 2. The influence coefficient for the doublet panel on itself is calculated separately as $C_{ii} = 1/2$.

A boundary condition based on the constant potential method (Dirichlet method) have been used. The velocity potential can be divided into a free stream potential, Φ_∞, and a perturbation potential, Φ [5]:

$$\Phi_i^* = (\Phi + \Phi_\infty)_i = constant \tag{3}$$

The influence coefficients represent the perturbation potential, Φ. The boundary condition, for panel element i, can then be written:

$$\sum_{j=1}^{N} B_{ij}\sigma_j + \sum_{j=1}^{N} C_{ij}\mu_j + \Phi_\infty + \sum_{l=1}^{N_W} C_{il}\mu_l = const \tag{4}$$

where j is the index notation for all the panel elements along the surface and l is for the wake panels. A second boundary condition, the Kutta condition i.e. a smooth flow at the sharp trailing edge, is needed to solve the problem:

$$(\mu_1 - \mu_N) + \mu_w = 0 \tag{5}$$

For the first timestep, there are $N + 1$ equations to be solved. This will increase with 1 for each time step, since the number of wake elements will be increasing with time.

2.2.5. Establishment of the RHS of the equation. The inner potential is selected to be equal to Φ_∞. The source strength is then [5]:

$$\sigma_j = \mathbf{n_j} \cdot \mathbf{Q}_\infty \tag{6}$$

where $\mathbf{n_j}$ is the local normal vector at panel element j, see Figure 6 and $\mathbf{Q}_\infty$ is the wind velocity vector. Equation 4 is reduced to:

$$\sum_{j=1}^{N} B_j\sigma_j + \sum_{j=1}^{N+1} C_j\mu_j + \sum_{l=1}^{N_W} C_l\mu_l = 0 \tag{7}$$

A linear algebraic equation is created for each collocation point along the surface of the body. The known parts of the equation are the influence coefficients, the source strengths and the

strength of the shedded wake elements. The strength of the first wake panel is however not known and is included in the doublet distribution of the airfoil. The Kutta condition (Equation 5) reduces the amount of unknowns to $N+1$. The doublet influence is rewritten such that:

$$A_{ij} = C_{ij}, \qquad j \neq 1, N \tag{8}$$
$$A_{i1} = C_{i1} - C_{iW}, \qquad j = 1 \tag{9}$$
$$A_{iN} = C_{iN} + C_{iW}, \qquad j = N \tag{10}$$

The source influence coefficients and source strengths are moved to the right hand side of the equation, and solved. This is only needed to be done once, and can be used for all time-steps as long as the shape of the body is constant. This is the RHS_s. For each time-steps a RHS_w vector containing the influence vector of the wake and the doublet strengths needs to be calculated. The RHS vector is established by adding RHS_s and RHS_w together.

$$RHS_s = -\sum_{j=1}^{N} B_j \sigma_j \tag{11}$$
$$RHS_w = -\sum_{l=1}^{N_W} C_l \mu_l \tag{12}$$
$$RHS = RHS_s + RHS_w \tag{13}$$

2.2.6. Solution of the linear set of equation. Following the steps above, one has the following matrix equation to be solved:

$$\begin{pmatrix} A_{11} & A_{12} & ... & A_{1N} \\ A_{21} & A_{22} & ... & A_{2N} \\ ... & ... & & ... \\ A_{N1} & A_{N2} & ... & A_{NN} \end{pmatrix} \begin{pmatrix} \mu_1 \\ \mu_2 \\ ... \\ \mu_N \end{pmatrix} = \begin{pmatrix} RHS_1 \\ RHS_2 \\ ... \\ RHS_N \end{pmatrix} \tag{14}$$

The strength of the doublets, μ_j can now be calculated. Based on this, the circulation can be calculated, which is used when calculating pressure and velocity.

2.2.7. Time-stepping procedure. For incompressible flows the instantaneous solution is independent of time derivatives. The steady-state solution techniques can therefore be used when solving time-dependent problems. As with steady-state flows the Kutta condition, Equation 5, is assumed valid [5].

In addition to the steps described above, the wake strength and its shape need to be considered. The strength of the element shed at the trailing edge is computed using the Kutta condition. The element is at later time steps convected downstream. It is assumed that the wake leaves the trailing edge at a mean angle. The wake should be parallel to the circulation vector, and this gives the necessary requirements to calculate the wake shape. By calculating the velocity induced by the singular elements and adding it to the free stream velocity, the propagation of the wake is estimated.

2.2.8. Secondary computations. The lift force of the blade section can be estimated from:

$$L = \rho U(t)\Gamma(t) + \rho \int_0^c \frac{\partial}{\partial t}\Gamma(x,t)dx \tag{15}$$

where ρ is the air density and Γ is the circulation. The circulation is calculated from the constant strength doublet panels. The constant doublet distribution is equivalent to two point vortices with opposite sign at the panel edges with opposite sign at the panel edges such that $\Gamma = -\mu$. [5]. The force normal to the rotor plane is:

$$N = L \cdot cos(\alpha + \gamma) \tag{16}$$

where α is the angle of attack and γ is the twist, see figure 4.

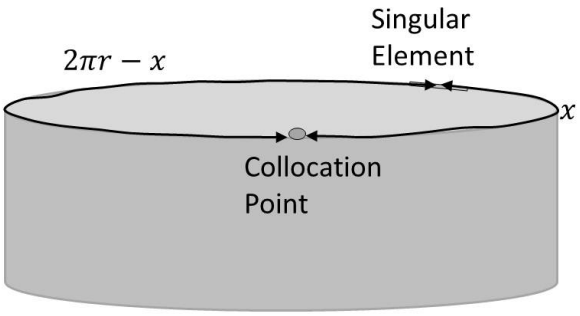

Figure 7. Distance from a singular element on a collocation point. The influence will be in two directions due to the circular path of the blades.

2.3. Adjacent airfoils and wakes
The airfoils are moving in a circular path when rotating about the wind turbine axis. The distance between the adjacent airfoils is $2\pi r/3$. The influence from both the neighbouring blades and their shed wake is included in the method. When the airfoil has moved a distance of one circumference, it will be at the same position as in the previous rotation (assuming no axial motion of the rotor). The shed wake will have moved a distance downstream.

As the airfoil moves away from the shed wake element, the influence from the wake panel becomes weaker. It will reach a point where the influence from the panel element is almost zero, before the influence starts increasing again. The collocation points at the airfoil will be influenced by the singular element in two different directions, as shown in figure 7. In this figure the distance to the singular element is x. The contribution of the influence in the opposite direction should however also bee included, even though it is at a larger distance from the collocation point. In Figure 7, this distance is $2\pi r - x$.

3. Validation
A validation of the code is presented in this section. As a first step the computed transient lift is compared to the Wagner function. Thereafter the lift coefficient of the airfoil at the blade section to be investigated later is compared to the tabulated data.

3.1. Wagner function
The resulting lift of a thin foil accelerating instantaneously from rest at $t = 0$ to a constant velocity U is given proportionally with the Wagner function [6]. Immediately, as the foil is accelerated, the lift is half of the lift at steady state. It increases monotonically towards the

steady-state lift. The simple vortex code is used to demonstrate the transient lift for a NACA 0012 airfoil at an angle of attack of 5 degrees. A comparison of the resulting transient lift coefficient is shown in figure 8.

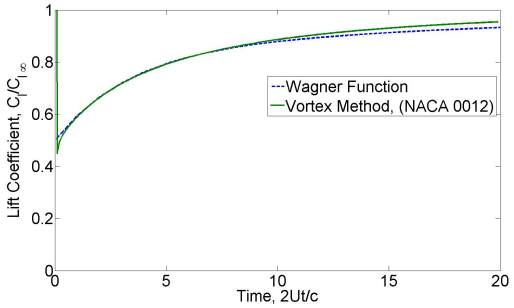

Figure 8. Comparison of the Wagner function and the vortex method.

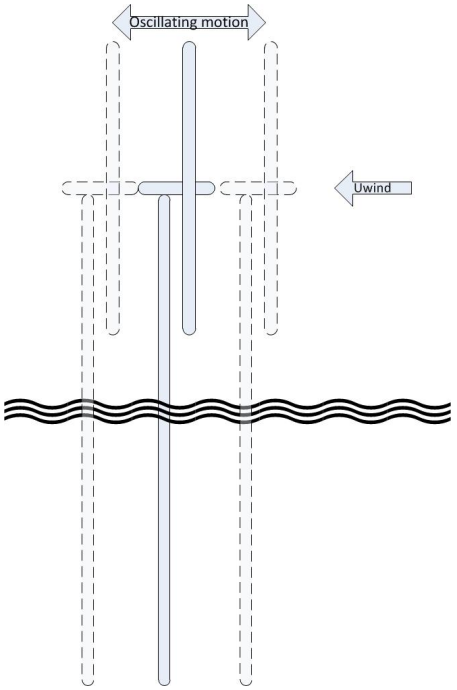

Figure 9. The oscillating motion of the floating wind turbine.

The Wagner function is based on a thin foil, and does not resemble an airfoil with thickness. The transient behavior of the lift force for the NACA 0012 is therefore expected not to behave exactly as the Wagner function predicts. Based on the figure, it is concluded that the method satisfactorily captures the transient behavior of the airfoil.

3.2. Airfoil properties

To ensure that the correct lift coefficients of the airfoil are found, and that a sufficient number of panels is used for the airfoil, the analyzed airfoil section will be compared with the lift coefficients for the airfoil given in the OC3 project [7]. It is the NACA64_A17 airfoil that has been analyzed. The vortex method developed is a time-dependent method, and the lift coefficient values will therefore steadily increase with time as the distance to the starting vortex increases. The values presented in table 1 are the lift coefficient with a dimensionless time coefficient of 20. The dimensionless time is defined as the distance traveled in semi-chords, $2Ut/c$.

There is a difference between the panel method and the tabulated lift coefficients. The difference is however relatively small.

4. Method

The pitch and yaw motions of the floating wind turbine will be contributing to the unsteady aerodynamics [4]. In our simplified 2D method we have investigated a surge motion as a simplified representation of the pitch motion. The surge motion is an axial motion of the wind turbine structure as shown in figure 9. In our simplified method only the flow in the cascade

Table 1. Validation of the airfoil lift coefficient for an angle of attack of 5 degrees

Angle of attack	OC3 [7]	panel method
5	1.011	0.998
6	1.103	1.106
7	1.181	1.213

Table 2. The main properties of the floating 5 MW wind turbine

Rating	5 MW
Rotor orientation, configuration	Upwind, 3 blades
Hub Height	90 m
Length of Blade	63 m
Cut-in, rated, cut-out wind speed	3m/s, 11.4 m/s, 25 m/s
Cut-out, rated rotor speed	6.9 rpm, 12.1 rpm
Rotor mass	110 000 kg
Nacelle mass	240 000 kg
Tower mass	347 460 kg
Platform mass	7 466 330 kg
Total wind turbine mass	8 163 790 kg

Table 3. Variables used in the simulation

Wind Speed	U_∞	6 m/s
Rotational Speed	Ω	7.955 rpm
Tip speed ratio	λ	9.63
Radius	r	44.55
Airfoil		NACA64_A17
Chord length	c	3.01 m

plane is considered and zero flow in the meridional plane, i.e. the 2-D method is not suited for a correct representation of the pitch motion.

The surge motion is investigated for a 5 MW floating spar type wind turbine. We will use the characteristics of the 5 MW wind turbine with a spar buoy platform as investigated by the OC3 project [8]. For simplicity there is no control system included, i.e. no pitching of the blades and fixed speed of the wind turbine. The main properties of the wind turbine are shown in table 2. The environmental conditions and wind turbine rotational speed used in the simulations are listed in table 3.

The airfoil coordinates are obtained from [9], and the rotor geometry from [7]. Only one of the nodes along the blade is used in the simulation. This node is located at 0.7R, where R is the total length of the blade.

The two dimensional blade is set up as shown in figure 4. The axial motion of the rotor is

included in the analysis by varying the incoming wind speed with time. An oscillation frequency period of 12 seconds, and an amplitude of 1.5 m, is used to represent the pitching behavior of a floating wind turbine.

5. Results

The results from the simulation are shown in figure 10 and in figure 11. At the start-up of the simulation, the transient lift due to the starting vortex when the airfoil is accelerated from zero can be seen in figure 10. To remove start-up effects from the results, the eight first rotations are removed from the result presented in the further analysis. In figure 11, the normal force on the oscillation rotor is presented as a function of the rotor axial velocity. The force is seen to follow an almost linear trend, that indicates that there is an aerodynamic damping effect. The linear coefficient, a, is -0.43 kN/(m/s), where the trend line is $y = ax + b$. The mean value of the normal force on the blade section presented in figure 11 is 2.74 kN. The angle of attack for this simulation ranges from 4.8 to 7.3 degrees.

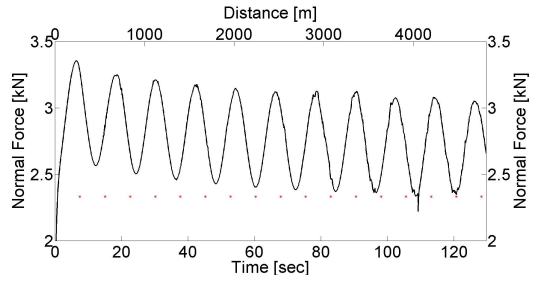

Figure 10. The computed normal force at the airfoil. The red dots indicate the rotations of the rotor

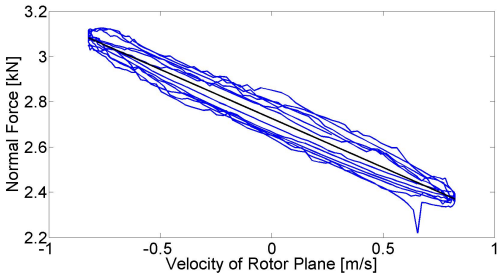

Figure 11. The normal force on the airfoil relative to the surge velocity.

6. Discussion

We would like to investigate analytically the aerodynamic damping quantified in the result section. Equation 16 shows the relation between the normal force and the lift force. For small values of the relative angle between the lift force component and the normal force component, the normal force is approximately equal to the lift force, $N \simeq L$.

The lift force can be expressed as:

$$\begin{aligned} L &= 1/2\rho U_{rel}^2 C_L(\alpha)c \\ &= 1/2\rho[(U-\dot{x})^2 + U_{rot}^2]C_L(\alpha)c \\ &= 1/2\rho[U^2 - 2U\dot{x} + \dot{x}^2 + U_{rot}^2]C_L(\alpha)c \\ &\simeq 1/2\rho[U^2 + U_{rot}^2]C_L(\alpha)c - \rho U\dot{x}C_L(\alpha)c \qquad (\dot{x}^2 \textit{ is assumed neglectable }) \end{aligned} \tag{17}$$

where ρ is the density of the air, U_{rel} is the relative wind speed, U is the wind speed, U_{rot} is the rotational speed of the blade, C_L is the lift coefficient and c is the chord length. The last term of Equation 17 is dependent on the velocity of the axial motion of the wind turbine, $\dot{x}$, but this is also true for the first term which contains the lift force coefficient, $C_L(\alpha)$. This coefficient is dependent upon the angle of attack, which will vary with the velocity of the wind turbine axial motion:

$$\alpha = atan(\frac{U-\dot{x}}{U_{rot}}) - \gamma \quad (18)$$

$$\alpha = \frac{U-\dot{x}}{U_{rot}} - \gamma \ \textit{(for small angles)} \quad (19)$$

where γ is the twist angle of the blade at the airfoil section. The lift coefficient as a function of the angle of attack can be linearized about the mean angle α_0:

$$\begin{aligned} C_L(\alpha) &= C_L(\alpha=\alpha_0) + \frac{\partial C_L}{\partial \alpha}\cdot\alpha_x \\ &= C_{L0} - \frac{\partial C_L}{\partial \alpha}\frac{\dot{x}}{U_{rot}} \end{aligned} \quad (20)$$

where α_0 is the mean angle of attack when $\dot{x}=0$. Combining Equations 17 and 20:

$$L \simeq 1/2\rho[U^2+U_{rot}^2](C_{L0} - \frac{\partial C_L}{\partial \alpha}\frac{\dot{x}}{U_{rot}})c - \rho U\dot{x}(C_{L0} - \frac{\partial C_L}{\partial \alpha}\frac{\dot{x}}{U_{rot}})c \quad (21)$$

which can be divided into four separate terms:

$$\begin{aligned} L_1 &= 1/2\rho[U^2+U_{rot}^2]C_{L0}c \\ L_2 &= -1/2\rho[U^2+U_{rot}^2]\frac{\partial C_L}{\partial \alpha}\frac{\dot{x}}{U_{rot}}c \\ L_3 &= -\rho U\dot{x}C_{L0}c \\ L_4 &= \rho U\dot{x}\frac{\partial C_L}{\partial \alpha}\frac{\dot{x}}{U_{rot}}c \end{aligned}$$

All data above is known for our simulation; ρ is 1.225 kg/m^3 and $\frac{\partial C_L}{\partial \alpha}$ is calculated from the values in table 1 as provided in [7]. A linearization between the values for 5^o and 7^o results in a $\frac{\partial C_L}{\partial \alpha}$ of 5.3 1/rad. C_{L0} is the lift force coefficient at 6^o. The last term L_4 is assumed much smaller compared to the other terms as $\dot{x}^2$ is a very small number. The term L_1 is the only one not dependent on the axial motion of the wind turbine, and is expected to have a mean value at 2.87 kN. The terms dependent on the axial motion of the wind turbine, $\dot{x}$, are L_2 and L_3. The sum of the two coefficients relating L_2 and L_3 to the axial motion is -0.39 kN/(m/s). If the calculations were based on the lift coefficients obtained by the panel vortex method, which are also given in table 1, the results would vary slightly. The stationary term, L_1 is then 2.88 kN, while the sum of the coefficients connecting to the axial velocity of the rotor is -0.46 kN/(m/s).

In our simulation, using the panel vortex method, these values are relatively close to the theoretically obtained values. Based on the simulations, the mean value was estimated to be 2.74 kN, and the term dependent on the velocity axial motion of the wind turbine was -0.43 kN/(m/s). The force component dependent on the axial velocity of the wind turbine motion is defined by the coefficient, c_a.

Since the aerodynamic damping coefficient c_a, connecting the surge velocity and the associated normal force, has a negative value it translates into a positive damping of the wind turbine structure. For airfoils closer to the hub, the change in the incoming velocity due to the axial rotor velocity will to a larger extent influence the relative wind velocity and the angle of the attack. This is in contrast to the outer blade sections where the aerodynamics is primarily governed by the rotational velocity. Correspondingly, for the blade sections closer to the hub, the motion-induced thrust will vary in a more complex manner with the axial rotor velocity forming a hysteresis rather than a straight line of the type shown in Figure 11.

7. Conclusion

The panel vortex method has been used to study the effect of the unsteady aerodynamics for floating wind turbines. The validity of the method is limited since it only considerers potential flow and only in the cascade plane. Since it is a potential flow code it is limited to modelling attached flow, and dynamic stall is therefore not modeled. The aerodynamic loads at lower angles of attack are however well estimated, and our result is limited to the range lower than the expected stall limit.

The aerodynamic damping coefficient for the surge motion was estimated for a blade segment on the rotor. This is valuable first step when looking at the aerodynamic effects of floating wind turbines. In the further work we will extend these two dimensional result to obtain the surge damping force on a full rotor.

References

[1] EWEA, "The european offshore wind industry key 2011 trends and statistics," tech. rep., European Wind Energy Association, 2012.
[2] Statoil, "Hywind." internet, accessed 27.09.2012. http://www.statoil.com/no/TechnologyInnovation/ NewEnergy/RenewablePowerProduction/Offshore/Hywind/Pages/HywindPuttingWindPowerToTheTest.aspx.
[3] J. Manwell, J. McGowan, and A. Rogers, *Wind Energy Explained*. John Wiley & Sons, 2009.
[4] T. Sebastian and M. A. Lackner, "Characterization of the unsteady aerodynamics of offshore floating wind turbines," *Wind Energy*, 2012.
[5] J. Katz and A. Plotkin, *Low-Speed Aerodynamics*. Cambridge University Press, 2001.
[6] J. G. Leishman, "Challenges in modelling the unsteady aerodynamics of wind turbines," *Wind Energy*, vol. 5, no. 2-3, pp. 85–132, 2002.
[7] J. Jonkman, S. Butterfield, W. Musial, and G. Scott, "Definition of a 5 MW Reference Wind Turbine," Technical Report NREL/TP-500-38050, National Renewable Energy Laboratory, Feburary 2009.
[8] J. Jonkman, T. Larsen, A. Hansen, T. Nygaard, K.Maus, M. Karimirad, Z. Gao, T. Moan, I. Fylling, J. Nichols, M. Kohlmeier, J. P. Vergara, D. Merino, W. Shi, and H. Park, "Offshore code comparison collaboration within iea wind task 23: Phase iv results regarding floating wind turbine modeling," in *European Wind Energy Conference (EWEC), Warsaw, Poland*, 20-23 April.
[9] J. Jonkman, "Nrel 5 MW Rotor Geometry." internet, accessed 27.09.2012. https://wind.nrel.gov/forum/wind/viewtopic.php?f=2&t=440.